Manta Ray Foraging Optimizer with Deep Learning-based Fundus Image Retrieval and Classification for Diabetic Retinopathy Grading

Syed Ibrahim Syed Mahamood Shazuli
Department of Computer and Information Sciences, Annamalai University, India
syedshazuli@yahoo.co.in

Arunachalam Saravanan
Department of Computer and Information Sciences, Annamalai University, India
vmahafx@gmail.com

Received: 25 July 2023 | Revised: 4 August 2023 | Accepted: 8 August 2023

 DOI: https://doi.org/10.48084/etasr.6226

ABSTRACT

Diabetic Retinopathy (DR) is a major source of sightlessness and permanent visual damage. Manual Analysis of DR is a labor-intensive and costly task that requires skilled ophthalmologists to observe and evaluate DR utilizing digital fundus images. The images can be employed for analysis and disease screening. This laborious task can gain a great advantage in automated detection by exploiting Artificial Intelligence (AI) techniques. Content-Based Image Retrieval (CBIR) approaches are utilized to retrieve related images in massive databases and are helpful in many application regions and most healthcare systems. With this motivation, this article develops the new Manta Ray Foraging Optimizer with Deep Learning-based Fundus Image Retrieval and Classification (MRFODL-FIRC) approach for the grading of DR. The suggested MRFODL-FIRC model investigates the retinal fundus imaging effectively to retrieve the relevant images and identify class labels. To achieve this, the MRFODL-FIRC technique uses Median Filtering (MF) as a pre-processing step. The Capsule Network (CapsNet) model is used to produce feature vectors with the MRFO algorithm as a hyperparameter optimizer. For the image retrieval process, the Manhattan distance metric is used. Finally, the Variational Autoencoder (VAE) model is used for recognizing and classifying DR. The investigational assessment of the MRFODL-FIRC technique is accomplished on medical DR and the outputs highlighted the improved performance of the MRFODL-FIRC algorithm over the current approaches.

Keywords-fundus images; image classification; diabetic retinopathy; deep learning; Manta Ray foraging optimization

I. INTRODUCTION

Diabetic Retinopathy (DR) denotes a complication of diabetes that happens due to damaged Blood Vessels (BVs) in the retina caused by higher blood sugar levels, leading to leaking and swelling in BV [1]. The vision can be completely lost in an advanced DR phase. Currently, ophthalmologists routinely use digital retinal fundus images for grading and classifying DR [2]. During this process, the ophthalmologist must visually observe digital fundus images, compare those with standard images such as EDTRS images, or images from archival DR image datasets, for interpreting images with more accuracy or for clarifying confusion [3]. This procedure is vulnerable to error or review fatigue and is a laborious process. The ophthalmologists find it difficult to use a large volume of past medical reports with proven pathology because they are not readily accessible to the historical medical reports that are appropriate to a new image that has to be identified [4]. Thus, the enormous quantity of diagnosis knowledge concealed in historical databases has been wasted [5].

Images can be medically relevant if they comprise similar kinds of lesions having the same visual appearance [6]. One method that has proved very beneficial in the early diagnosis of retinal diseases is the CBIR method. The fundus images obtained from many diabetic patients are useful data for analysing retinal diseases with the help of image processing methods. The CBIR process has two stages in it [7], the feature extraction stage and the query matching stage. In the first stage, a feature vector is generated by extracting features like texture, color, and shape of images. Feature vector is an optimized form of imagery [8]. Query matching depends on similarity measurement, which makes use of the distance of the query from all images in the database to detect the closest image. It is a time-consuming process if done manually, it needs significant effort, and may lead to misdiagnosis [9]. Hence, to reduce the overall cost and avoid misdiagnosis, time, and effort,

Computer-Aided Detection (CAD) methods can be used as potential means. In the past, Deep Learning (DL) techniques have been applied in several domains, including medical image analysis [10]. DL has the potential to detect features precisely from input datasets for segmentation or classification and normally outpaces all classical image analysis methods.

In the current study, the new Manta Ray Foraging Optimizer with Deep Learning based Fundus Image Retrieval and Classification (MRFODL-FIRC) approach for the grading of DR. The presented MRFODL-FIRC approach exploits Median Filtering (MF) as a pre-processing step. The Capsule Network (CapsNet) model is used to produce feature vectors with the MRFO algorithm as a hyperparameter optimizer. For the image retrieval process, the Manhattan distance metric is used. Finally, the Variational Autoencoder (VAE) model is used for recognizing and classifying DR. The investigational assessment of the MRFODL-FIRC technique is accomplished on a medical DR dataset.

II. RELATED WORKS

Authors in [11] introduced the new diabetic retinopathy screening algorithm utilizing an asymmetric DL feature. Through U-Net for BV segmentation and optic disc, the asymmetric DL features were derived. For the DR lesion classification, a CNN with an SVM was utilized. The lesions were categorized into 4 classes, i.e. haemorrhages, normal, exudates, and microaneurysms. Author in [12], presented a two-step training approach using a supervised contrastive loss function called SCL technique for identifying the DR and its robust phases from fundus image. The pre-trained Xception CNN method was deployed as the encoder with TL and the CLAHE model was implemented to enrich the image quality. The SNE technique was utilized to visualize embedding space made up of 128D space into 2D space to interpret the SCL model. Authors in [13] suggested a dual-phase technique for the automatically classification of DR. Due to the lower fraction of positive samples in the BV and asymmetric Optic Disk (OD) detection system, data augmentation and pre-processing methods were utilized for enriching the image quantity and quality. The first step utilized 2 U-Net approaches for OD and BV segmentation. After pre-processing, the symmetric fusion CNN-SVD algorithm was employed to choose and extract the discriminative factors followed by BV and OD extraction through InceptionV3 depending on TL. Authors in [14] introduced ML-CAD systems that visualized the pathological variations and identified DR images. Firstly, the authors reduced noise, standardized the size, and enhanced the quality of the retinal images. Then, by computing the gray-level average of run length matrix in 4 diverse directions, the authors distinguished between the DR and healthy cases with the help of a DL method (UNet). The system mechanically derived 4 major classes: haemorrhages, BVs, microaneurysms, and exudates.

Authors in [15] presented a DL-related technique for automatically evaluating DR in retina FIs. For increasing the discriminative capability of the retrieved features, a multi-scale attention system was implemented in a deep CNN structure. A brand-new loss function termed modified grading loss was provided that boosts the training convergence of the suggested method by considering the distance between different grades of various DR categories. Authors in [16] devised an innovative technique for precise haemorrhage detection from retinal images. Initially, this technique makes use of the contrast advancement approach to enrich the edge information from input fundus imaging. Next, an innovative CNN structure was devised for identifying haemorrhages. An adapted pretrained CNN technique was utilized for extracting features from identified haemorrhages. In stage 3, each extracted feature vector was merged through the convolutional sparse image decomposition algorithm.

III. THE PROPOSED MODEL

In this research, an automatic DR grading and classification model, named the MRFODL-FIRC technique is developed. The proposed MRFODL-FIRC technique examines retinal fundus images efficaciously for retrieving related images and determining the classes. It encompasses different sub-processes, namely MF-based pre-processing, CapsNet-based feature extracting process, MRFO-based tuning process, Manhattan distance-based similarity measurement, and VAE classification. Figure 1 demonstrates the comprehensive flow of the MRFODL-FIRC model.

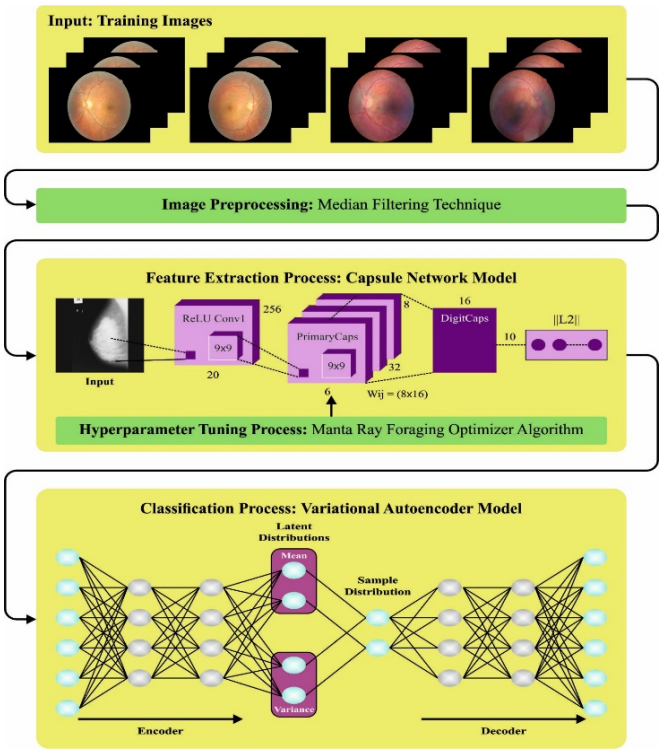

Fig. 1. Overall flow of the MRFODL-FIRC approach.

A. MF-based Preprocessing

At first, the MF technique is used to pre-process the fundus images. MF is a procedure utilized to remove noise in the image [17]. This mechanism is exchanging all the pixels from the image with the median value of their neighboring pixels. The simple steps contained in MF are:

- Select the size of filter window: This window is classically a square or rectangular region centred in the pixel being filtered.
- Slide the filter window on the image: The filtering window is then slid on the image, one pixel at a time.
- Compute the median value: the median value of the pixel in the filter window can be computed for every pixel of the image.
- Exchange the pixel with the median value: The pixel being filtered is then exchanged by the computed median value.

B. Feature Extraction using the CapsNet Model

To produce feature vectors, the CapsNet model is utilized. CapsNet is a kind of NN which contains a set of neurons from which activity vectors point out the instantiate parameter of a specific entity [18], for instance, an object or object portion. It integrates 2 convolution layers with an entirely associated layer (termed as RecCaps). The 1st layer is utilized for converting the character images of the input as activation blocks. The second layer performs as PrimaryCaps. The modification of "neurons" with a singular scalar output was completed to PrimaryCaps with an 8-dimension vector procedure. Lastly, the the RecCaps layer is utilized for encapsulating the spatial connection amongst every local feature in the PrimaryCaps. Afterwards every feature can be provided as a superior dimension advanced capsule taking a dimension of 16. During the final layers, this method utilizes a nonlinear "squashing" activation function for ensuring the decrease of vector lengths from 0 to 1. This formula demonstrated provides the resultant vector of capsule j.

$$Y_m = \frac{\|X_m\|^2}{1+\|X_m\|^2}\frac{X_m}{\|X_m\|} \quad (1)$$

where Y_m signifies the resultant vector for capsule m and X_m denotes the input vector.

Accordingly, the length of the capsule's resultant vector is utilized for representing the possibility of recovered local features. The lower-level factors in the input character can be removed by the first layer termed as $Conv1$. Afterwards, the primary capsule layer is utilized for applying convolution functions on the chosen group of features for acquiring 3D matrices. The dimensions of the matrices are 18×16×128 and lastly, the matrices are gathered as 16 capsules. Each matrix has dimensions of 18×16×8. An overall of 4680 capsules can be attained by utilizing squashing activation function once the stacking and flattening of capsules are completed. The extraction feature f_n is signified as 8-dimension vectors for each capsule.

The dynamic routing technique was utilized for recognizing a part of PrimaryCaps that is highly co-relatable with advanced capsules which determine the local features which are best probably connected to higher-level features. This procedure supports creating a model added to spatial connection needed for interpreting and detecting handwritten words. For every iteration, the coupling coefficient can be computed. Afterwards, the resultant vector for the capsule of the subsequent layer can be calculated. Lastly, the sum of agreements among every capsule proceeds to the last outcome obtained.

C. Hyperparameter Tuning with the MRFO Algorithm

In this work, the MRFO algorithm adjusts the hyperparameters of the CapsNet model. Authors in [19] proposed MRFO as a nature-inspired metaheuristic that was applied to resolve different optimization issues [19]. The primary motivation of the MRFO derives from the behavior of Manta Rays (MRs) when capturing food. Somersault foraging, chain foraging, and cyclone foraging are the 3 major foraging approaches in the MRFO algorithm.

1) Chain Foraging

In this phase, MRs start foraging by moving sequentially and forming head-to-tail chains. Apart from the first individual, the others move towards the food and nearby MRs for cooperation. The chain foraging can be mathematically modelled as:

$$p_i^{t+1} = \begin{cases} p_i^t + r.(p_{Best} - p_i^t) + \alpha.(p_{Best} - p_i^t), i = 1 \\ p_i^t + r.(p_{i-1}^t - p_i^t) + \alpha.(p_{Best} - p_i^t), i = 2, \dots, N \end{cases} \quad (2)$$

$$\alpha = 2.r.\sqrt{\log(r)} \quad (3)$$

In (2), p_i^t signifies the i-th individual location at t iteration, r denotes a randomly generated integer within [0,1], α denotes a weighted coefficient and p_{Best} signifies the optimum found location.

2) Cyclone Foraging

This approach is considered as the spiral displacement of MRs towards the prey as follows:

$$p_i^{t+1} = \begin{cases} p_i^t + r.(p_{Best} - p_i^t) + \beta.(p_{Best} - p_i^t), i = 1 \\ p_i^t + r.(p_{i-1}^t - p_i^t) + \beta.(p_{Best} - p_i^t), i = 2, \dots, N \end{cases} \quad (4)$$

$$p_{rand} = Lb + r.(Ub - Lb) \quad (5)$$

$$p_i^{t+1} = \begin{cases} p_i^t + r.(p_{rand} - p_i^t) + \beta.(p_{rand} - p_i^t), i = 1 \\ p_i^t + r.(p_{i-1}^t - p_i^t) + \beta.(p_{rand} - p_i^t), i = 2, \dots, N \end{cases} \quad (6)$$

$$\beta = 2.e^{(r_1\frac{T-t+1}{T})}.\sin(2.\pi.r_1) \quad (7)$$

where T shows the maximal number of iterations, p_{rand} characterizes a randomized location in the space defined by lower and higher boundaries Lb and Ub, β represents a weight coefficient, and r_1 denotes a random value within [0,1].

3) Somersault Foraging

In such cases, the location of the prey is represented as a pivot. The MRs will be swimming toward the food and somersault to the newest location:

$$p_i^{r+1} = p_i^t + S.(r_2.p_{Best} - r_3.p_i^t), i = 1, \dots, N \quad (8)$$

where S characterizes the somersault feature set to 2, r_2 and r_3 are randomly generated numbers within [0,1]. The MRFO manner produces a Fitness Function (FF) for classification. The minimized classifier error rate is:

$$fitness(x_i) = ClassifierErrorRate(x_i)$$
$$= \frac{number\ of\ misclassified\ samples}{Total\ number\ of\ samples} * 100 \quad (9)$$

4) Similarity Measurement

The Manhattan distance metric was used for the image retrieval process. Manhattan distance is a metric whereas the distance between 2 points is the total of the absolute variances of Cartesian co-ordinates [20]:

$$d = |p_1 - q_1| + |p_2 - q_2| \quad (10)$$

and the generalization equation to n-dimensional space is expressed as:

$$D_m = \sum_{i=1}^{n} |p_i - q_i| \quad (11)$$

whereas, n denotes the number of dimensions and p_i, q_i are data points.

5) Image Classification using VAE

At the final stage, the VAE model is utilized for the image classification process. An Auto-Encoder (AE) is an NN which is given the training to try to duplicate its input to output [21]. The Hidden Layer (HL) h defines the code utilized for representing the input. The network could be observed as containing two parts like the encoded function $z = f(x)$ and decoding generates a reconstruction $g(z)$, where x implies the input dataset. One method to attain suitable features in the AE is to make z have lesser dimension than x. The AE code dimension number is lower than the input dimensional and is termed complete. For generating an instance in the method, the VAE primary draws the z instance in the code distribution $p_{model}(z)$. An instance is run over by a differentiable generator network (z). Eventually, x has a distribution $p_{model}(x,\cdot g(z)) = p_{model}(x|z)$. In the trained method, the approximate inference network (or encoded) $q(zx)$ is utilized for obtaining z and p_{model} (xz) is observed as a decoded network. The main insight behind VAEs is that it is trained by maximizing the variational lower bounds $L(q)$ connected to x data points:

$$L(q) = E_{z\sim q(z|x)} \log p_{model}(z,x) + H\big(q(z|x)\big) \quad (12)$$
$$= E_{z\sim q(z|x)} \log p_{model}(x|z) - D_{KL}(q(z|x)||p_{model}(z)) \quad (13)$$

Equation (12) distinguishes the first term as the joint log possibility of hidden and visible variables in the estimated hidden variable posterior. If q has a Gaussian distribution with noise and mean value, it maximizes the entropy term and stimulates enhancing the Standard Deviation (SD). Usually, the entropy term stimulates the variational posterior to locate the maximum possibility mass on the z value which is created as x, instead of disintegrating toward a singular point evaluation of probable value. The network defined in (13) is the same. The "reparameterization trick" is used for moving the sample towards the input layers. After computing $p_{model}z = \mu(x) + \theta^{1/2}(x) * e$, its instance in $N(\mu(x), \theta(x))$ by sample $\sim N(0, I)$,. $\mu(x)$ and $\theta(x)$ denotes the mean and co-variance of $(z|x)$. Therefore, (13) is measured as follows:

$$L(q) = E_{\epsilon\sim N(0,I)} p_{model}(x|z = \mu(x) + \theta^{\frac{1}{2}}(x) \times \epsilon) - D_{KL}(q(z|x)||p_{model}(z)) \quad (14)$$

VAE contains multiple AE, input, and output layers. Every AE layer has been trained individually in an unsupervised method, and the outcome of HL in the preceding AE was utilized as input to the subsequent layer. The supervised fine-tuning stage was executed in order to learn the overall parameters of the network utilizing the BP system. This model contains five HLs, one input layer, and one output layer. In Figure 2, the overall confusion matrix of the MRFODL-FIRC method on the DR classification process is illustrated. The outcome shows that the MRFODL-FIRC method gains effectual identification of DR over the existing approaches.

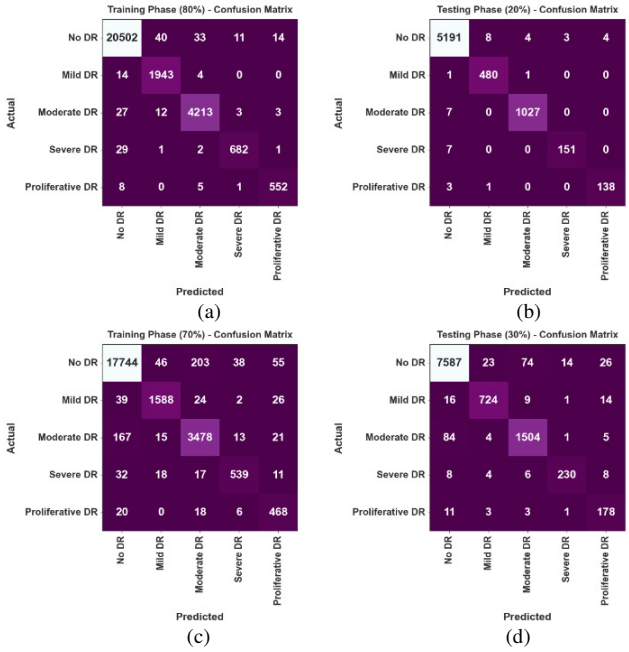

Fig. 2. Confusion matrices of MRFODL-FIRC method (a)-(b) 80:20 and (c)-(d) 70:30 of TRP/TSP.

IV. PERFORMANCE VALIDATION

The suggested technique was simulated by employing Python 3.6.5 on PC i5-8600k, 250GB SSD, GeForce 1050Ti 4GB, 16GB RAM, and 1TB HDD. The parameter set up is: learning rate: 0.01, activation: ReLU, epoch count: 50, dropout: 0.5, and batch size: 5.

The detailed classification output of the MRFODL-FIRC approach on 80:20 of TRP/TSP is shown in Table I. The obtained output infers the effectual identification of different DR stages. As a sample, on 80% of TRP, the MRFODL-FIRC approach obtains an average $accu_y$ of 99.70%, $prec_n$ of 98.12%, $reca_l$ of 98.09%, F_{score} of 98.10%, and AUC_{score} of 98.89%. Alongside, on 20% of TSP, the MRFODL-FIRC methodology attains an average $accu_y$ of 99.78%, $prec_n$ of 98.51%, $reca_l$ of 98.26%, and F_{score} of 98.38%, and AUC_{score} of 99.00%. In Table II, the detailed classification output of the MRFODL-FIRC approach on 70:30 of TRP/TSP is shown. The attained output infers the effectual identification of different DR stages. For instance, on 70% of TRP, the MRFODL-FIRC approach obtains an average $accu_y$ of 98.75%, $prec_n$ of

91.50%, $reca_l$ of 93.12%, F_{score} of 92.24%, and AUC_{score} of 95.93%. On 30% of TSP, the MRFODL-FIRC method obtains an average $accu_y$ of 98.80%, $prec_n$ of 91.68%, $reca_l$ of 93.55%, and F_{score} of 92.50%, and AUC_{score} of 96.15%.

TABLE I. CLASSIFICATION OUTPUT OF MRFODL-FIRC MODEL ON 80:20 OF TRP/TSP

Class	$Accu_y$	$Prec_n$	$Reca_l$	F_{score}	AUC_{score}
Training Phase (80%)					
No DR	99.37	99.62	99.52	99.57	99.24
Mild DR	99.75	97.34	99.08	98.21	99.44
Moderate DR	99.68	98.97	98.94	98.95	99.38
Severe DR	99.83	97.85	95.38	96.60	97.66
Proliferative DR	99.89	96.84	97.53	97.18	98.73
Average	99.70	98.12	98.09	98.10	98.89
Testing Phase (20%)					
No DR	99.47	99.65	99.64	99.64	99.32
Mild DR	99.84	98.16	99.59	98.87	99.72
Moderate DR	99.83	99.52	99.32	99.42	99.62
Severe DR	99.86	98.05	95.57	96.79	97.76
Proliferative DR	99.89	97.18	97.18	97.18	98.56
Average	99.78	98.51	98.26	98.38	99.00

TABLE II. CLASSIFICATION OUTPUT OF MRFODL-FIRC MODEL ON 70:30 OF TRP/TSP

Class	$Accu_y$	$Prec_n$	$Reca_l$	F_{score}	AUC_{score}
Training Phase (70%)					
No DR	97.56	98.57	98.11	98.34	97.07
Mild DR	99.31	95.26	94.58	94.92	97.12
Moderate DR	98.06	92.99	94.15	93.57	96.45
Severe DR	99.44	90.13	87.36	88.72	93.56
Proliferative DR	99.36	80.55	91.41	85.64	95.47
Average	98.75	91.50	93.12	92.24	95.93
Testing Phase (30%)					
No DR	97.57	98.46	98.23	98.34	97.00
Mild DR	99.30	95.51	94.76	95.14	97.21
Moderate DR	98.23	94.24	94.12	94.18	96.54
Severe DR	99.59	93.12	89.84	91.45	94.84
Proliferative DR	99.33	77.06	90.82	83.37	95.15
Average	98.80	91.68	93.55	92.50	96.15

TABLE III. OUTPUT COMPARISON OF THE MRFODL-FIRC MODEL WITH EXISTING APPROACHES

Methods	$Accu_y$	$Prec_n$	$Reca_l$	F_{score}
WFDLN	98.00	95.29	94.70	95.11
AlexNet	89.50	90.87	91.60	91.52
MobileNet	92.90	93.28	93.12	93.46
Xception	92.80	92.33	92.93	92.75
ResNet-50	94.51	95.13	95.33	95.14
MRFODL-FIRC	99.78	98.51	98.26	98.38

Table III demonstrates the comprehensive comparison of the MRFODL-FIRC approach with recent approaches. The results demonstrate the enhanced performance of the MRFODL-FIRC technique with increasing $accu_y$ and F_{score} values. Based on $accu_y$, the MRFODL-FIRC technique reaches an improving $accu_y$ of 99.78% while the AlexNet, MobileNet, Xception, and ResNet-50 approaches obtain lesser $accu_y$ values. The MRFODL-FIRC technique reaches an improved F_{score} of 98.38% while the AlexNet, MobileNet, Xception, and ResNet50 models obtain smaller F_{score} values. These outputs confirm the enhanced achievement of the MRFODL-FIRC approach over the rest of the currently used methods.

V. CONCLUSION

In this research, an automatic DR grading and classification model, named MRFODL-FIRC is proposed. The presented MRFODL-FIRC technique examined the retinal fundus images efficaciously for retrieving related images and determining classes. It encompasses different sub-processes namely CapsNet-based feature extraction, MF-based pre-processing, MRFO-based tuning process, Manhattan distance-based similarity measuring, and VAE classification. The experimental assessment of the MRFODL-FIRC technique was conducted on a medical DR dataset and the outputs highlighted the improved performance of the MRFODL-FIRC technique over the currently used techniques. Therefore, the presented MRFODL-FIRC technique is useful for effectual retrieving and classification of retinal images. In the future, the MRFODL-FIRC method can be boosted by a deep instance segmenting process. Besides, the computation complexity of the proposed model needs to be investigated.

REFERENCES

[1] L. K. Singh, M. Khanna, S. Thawkar, and R. Singh, "Collaboration of features optimization techniques for the effective diagnosis of glaucoma in retinal fundus images," *Advances in Engineering Software*, vol. 173, Nov. 2022, Art. no. 103283, https://doi.org/10.1016/j.advengsoft.2022.103283.

[2] G. Kalyani, B. Janakiramaiah, A. Karuna, and L. V. N. Prasad, "Diabetic retinopathy detection and classification using capsule networks," *Complex & Intelligent Systems*, vol. 9, no. 3, pp. 2651–2664, Jun. 2023, https://doi.org/10.1007/s40747-021-00318-9.

[3] M. Sahoo, S. Ghorai, M. Mitra, and S. Pal, "Improved detection accuracy of red lesions in retinal fundus images with superlearning approach," *Photodiagnosis and Photodynamic Therapy*, vol. 42, Jun. 2023, Art. no. 103351, https://doi.org/10.1016/j.pdpdt.2023.103351.

[4] G. Saxena, D. K. Verma, A. Paraye, A. Rajan, and A. Rawat, "Improved and robust deep learning agent for preliminary detection of diabetic retinopathy using public datasets," *Intelligence-Based Medicine*, vol. 3–4, Dec. 2020, Art. no. 100022, https://doi.org/10.1016/j.ibmed.2020.100022.

[5] M. S. Farooq *et al.*, "Untangling Computer-Aided Diagnostic System for Screening Diabetic Retinopathy Based on Deep Learning Techniques," *Sensors*, vol. 22, no. 5, Jan. 2022, Art. no. 1803, https://doi.org/10.3390/s22051803.

[6] H. Fu *et al.*, "A Deep Learning System for Automated Angle-Closure Detection in Anterior Segment Optical Coherence Tomography Images," *American Journal of Ophthalmology*, vol. 203, pp. 37–45, Jul. 2019, https://doi.org/10.1016/j.ajo.2019.02.028.

[7] V. D. Vinayaki and R. Kalaiselvi, "Multithreshold Image Segmentation Technique Using Remora Optimization Algorithm for Diabetic Retinopathy Detection from Fundus Images," *Neural Processing Letters*, vol. 54, no. 3, pp. 2363–2384, Jun. 2022, https://doi.org/10.1007/s11063-021-10734-0.

[8] K. Aldriwish, "A Deep Learning Approach for Malware and Software Piracy Threat Detection," *Engineering, Technology & Applied Science Research*, vol. 11, no. 6, pp. 7757–7762, Dec. 2021, https://doi.org/10.48084/etasr.4412.

[9] N. B. Serradj, A. D. K. Ali, and M. E. A. Ghernaout, "A Contribution to the Thermal Field Evaluation at the Tool-Part Interface for the Optimization of Machining Conditions," *Engineering, Technology & Applied Science Research*, vol. 11, no. 6, pp. 7750–7756, Dec. 2021, https://doi.org/10.48084/etasr.4235.

[10] S. Nuanmeesri, "A Hybrid Deep Learning and Optimized Machine Learning Approach for Rose Leaf Disease Classification," *Engineering,*

Technology & Applied Science Research, vol. 11, no. 5, pp. 7678–7683, Oct. 2021, https://doi.org/10.48084/etasr.4455.

[11] P. K. Jena, B. Khuntia, C. Palai, M. Nayak, T. K. Mishra, and S. N. Mohanty, "A Novel Approach for Diabetic Retinopathy Screening Using Asymmetric Deep Learning Features," *Big Data and Cognitive Computing*, vol. 7, no. 1, Mar. 2023, Art. no. 25, https://doi.org/10.3390/bdcc7010025.

[12] M. R. Islam *et al.*, "Applying supervised contrastive learning for the detection of diabetic retinopathy and its severity levels from fundus images," *Computers in Biology and Medicine*, vol. 146, Jul. 2022, Art. no. 105602, https://doi.org/10.1016/j.compbiomed.2022.105602.

[13] A. Bilal, L. Zhu, A. Deng, H. Lu, and N. Wu, "AI-Based Automatic Detection and Classification of Diabetic Retinopathy Using U-Net and Deep Learning," *Symmetry*, vol. 14, no. 7, Jul. 2022, Art. no. 1427, https://doi.org/10.3390/sym14071427.

[14] E. Abdelmaksoud, S. El-Sappagh, S. Barakat, T. Abuhmed, and M. Elmogy, "Automatic Diabetic Retinopathy Grading System Based on Detecting Multiple Retinal Lesions," *IEEE Access*, vol. 9, pp. 15939–15960, 2021, https://doi.org/10.1109/ACCESS.2021.3052870.

[15] M. T. Al-Antary and Y. Arafa, "Multi-Scale Attention Network for Diabetic Retinopathy Classification," *IEEE Access*, vol. 9, pp. 54190–54200, 2021, https://doi.org/10.1109/ACCESS.2021.3070685.

[16] S. Maqsood, R. Damaševičius, and R. Maskeliūnas, "Hemorrhage Detection Based on 3D CNN Deep Learning Framework and Feature Fusion for Evaluating Retinal Abnormality in Diabetic Patients," *Sensors (Basel, Switzerland)*, vol. 21, no. 11, Jun. 2021, Art. no. 3865, https://doi.org/10.3390/s21113865.

[17] A. Noor, Y. Zhao, R. Khan, L. Wu, and F. Y. O. Abdalla, "Median filters combined with denoising convolutional neural network for Gaussian and impulse noises," *Multimedia Tools and Applications*, vol. 79, no. 25, pp. 18553–18568, Jul. 2020, https://doi.org/10.1007/s11042-020-08657-4.

[18] A. Moudgil, S. Singh, V. Gautam, S. Rani, and S. H. Shah, "Handwritten devanagari manuscript characters recognition using capsnet," *International Journal of Cognitive Computing in Engineering*, vol. 4, pp. 47–54, Jun. 2023, https://doi.org/10.1016/j.ijcce.2023.02.001.

[19] A. Moudgil, S. Singh, V. Gautam, S. Rani, and S. H. Shah, "Handwritten devanagari manuscript characters recognition using capsnet," *International Journal of Cognitive Computing in Engineering*, vol. 4, pp. 47–54, Jun. 2023, https://doi.org/10.1016/j.ijcce.2023.02.001.

[20] N. E. M. Isa, A. Amir, M. Z. Ilyas, and M. S. Razalli, "The Performance Analysis of K-Nearest Neighbors (K-NN) Algorithm for Motor Imagery Classification Based on EEG Signal," *MATEC Web of Conferences*, vol. 140, 2017, Art. no. 01024, https://doi.org/10.1051/matecconf/201714001024.

[21] M. Dai, D. Zheng, R. Na, S. Wang, and S. Zhang, "EEG Classification of Motor Imagery Using a Novel Deep Learning Framework," *Sensors (Basel, Switzerland)*, vol. 19, no. 3, Jan. 2019, Art. no. 551, https://doi.org/10.3390/s19030551.